PASJ: Publ. Astron. Soc. Japan **59**, S779–S784, 2007 November 30

Hinode Observations of a Vector Magnetic Field Change Associated with a Flare on 2006 December 13*

Masahito KUBO,[1,2] Takaaki YOKOYAMA,[3] Yukio KATSUKAWA,[4] Bruce LITES,[1] Saku TSUNETA,[4] Yoshinori SUEMATSU,[4] Kiyoshi ICHIMOTO,[4] Toshifumi SHIMIZU,[2] Shin'ichi NAGATA,[5] Theodore D. TARBELL,[6] Richard A. SHINE,[6] Alan M. TITLE,[6] and David ELMORE[1]

[1]*High Altitude Observatory, National Center for Atmospheric Research,† P O Box 3000, Boulder, CO 80307, USA*
kubo@ucar.edu

[2]*Institute of Space and Astronautical Science, Japan Aerospace Exploration Agency, 3-1-1 Yoshinodai, Sagamihara, Kanagawa 229-8510*

[3]*Department of Earth and Planetary Science, School of Science, The University of Tokyo, 7-3-1 Hongo, Bunkyo-ku, Tokyo 113-0033*

[4]*National Astronomical Observatory of Japan, 2-21-1 Osawa, Mitaka, Tokyo 181-8588*

[5]*Hida Observatory, Kyoto University, Takayama, Gifu 506-1314*

[6]*Lockheed Martin Solar and Astrophysics Labratory, Building 252, 3251 Hanover St., Palo Alto, CA 94304, USA*

(Received 2007 June 27; accepted 2007 September 14)

Abstract

Continuous observations of the flare productive active region 10930 were successfully carried out with the Solar Optical Telescope aboard the Hinode spacecraft during 2006 December 6 to 19. We focused on the evolution of photospheric magnetic fields in this active region, and the magnetic field properties at the site of the X3.4 class flare, using a time series of vector field maps with high spatial resolution. The X3.4 class flare occurred on 2006 December 13 at the apparent collision site between the large, opposite polarity umbrae. Elongated magnetic structures with alternatingly positive and negative polarities resulting from flux emergence appeared one day before the flare in the collision site penumbra. Subsequently, the polarity inversion line at the collision site became very complicated. The number of bright loops in Ca II H increased during the formation of these elongated magnetic structures. Flare ribbons and bright loops evolved along the polarity inversion line and one footpoint of the bright loop was located in a region having a large departure of the field azimuth angle with respect to its surroundings. SOT observations with high spatial resolution and high polarization precision revealed temporal change in the fine structure of magnetic fields at the flare site: some parts of the complicated polarity inversion line then disappeared, and in those regions the azimuth angle of the photospheric magnetic field changed by about 90°, becoming more spatially uniform within the collision site.

Key words: Sun: flares — Sun: magnetic fields — Sun: photosphere — Sun: sunspots

1. Introduction

What magnetic activity of the photosphere is responsible for triggering solar flares? Many studies have attempted to address this question through measurements of the evolution of photospheric magnetic fields associated with flares. Major flares most often occur around the sheared polarity inversion line in complicated active regions. Precision measurements of the magnetic field vector with high spatial resolution are necessary to reveal changes in its fine structure at the flare site, and also to minimize the inference of spurious magnetic cancellation events. Moreover, continuous observations under stable conditions, and for long duration are crucial for understanding formation of the sheared polarity inversion line [i.e., for study of the energy storage process, see papers cited in Priest and Forbes (2002)].

Because Hinode satellite (Kosugi et al. 2007) is in a sun-synchronous polar orbit, it observes the Sun continuously for eight months each year without any interruption by spacecraft night. The Solar Optical Telescope (SOT: Tsuneta et al. 2007; Suematsu et al. 2007; Ichimoto et al. 2007; Shimizu et al. 2007a) aboard Hinode is a unique facility that has the capability of providing a long sequence of vector magnetic field measurements at high spatial resolution. Thus, a primary objective of Hinode/SOT is to obtain flare-related changes in the magnetic field under seeing-free conditions. In this paper, we present an initial report on the evolution of the active region 10930 producing 4 X-class flares and magnetic field, and discuss the properties of the field and the chromospheric emission at the flare site.

2. Observation and Data Analysis

In 2006 December, three X-class flares (X6.5 on December 6, X3.4 on December 13, and X1.5 on December 14) were observed with SOT. In this paper we focus on the X3.4 flare on December 13, and on the associated evolution of the active

* Movies 1 and 2 are available at ⟨http://pasj.asj.or.jp/v59/sp3/59s331/⟩.

† The National Center for Atmospheric Research is sponsored by the National Science Foundation.

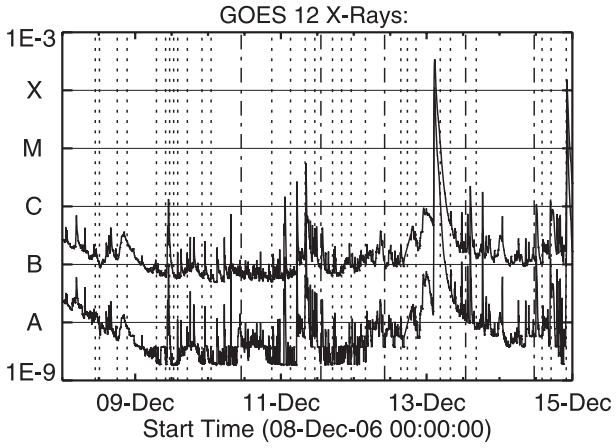

Fig. 1. Time profiles of the X-ray flux from the GOES 12 satellite from 2006 December 8 to 15. The upper and lower solid profiles indicate the full Sun solar X-ray output in the 1–8 Å and 0.5–4.0 Å passbands, respectively. The vertical dotted lines (dot-dashed lines) represent the start time of the slit scanning for Fast Map (Normal Map) with the SOT/SP.

region from December 8 to 15, while the active region was located not too far from the disk center. For much of this period, SOT simultaneously obtained the following data: the Broadband Filter Imager (BFI) provided G-band 4305 Å and Ca II H 3968 Å images, and the Narrowband Filter Imager (NFI) provided longitudinal magnetograms in the photosphere. The time cadence of the BFI and NFI is 2 minutes. The field of view was $218'' \times 109''$ with a pixel size of $0.''108$ for the BFI and $327'' \times 164''$ with pixel size of $0.''16$ for the NFI (these data are binned 2×2 pixels from the full resolution). The Spectro-Polarimeter (SP) obtained the full polarization state (I, Q, U, and V) of two magnetically sensitive Fe lines at 6301.5 Å and 6302.5 Å with wavelength sampling of 21.6 mÅ. The spatial distribution of magnetic field vectors over an active region may be obtained by a scanning the solar image over the SP slit. Figure 1 shows the GOES time variation of full Sun X-ray flux. Also indicated in figure 1 are the start times of SP mapping observations in two observing modes (Normal Map and Fast Map). The spatial sampling was $0.''148 \times 0.''159$ and the integration time for each slit position was 4.8 s for the Normal Map mode. The spatial sampling of the Fast Map mode was $0.''295 \times 0.''317$ and the integration time was 3.2 s.

The observation of full Stokes profiles permits us to derive accurate, quantitative measures of the magnetic field vector in the photosphere. We used a non-linear least-squares fitting technique to fit analytical Stokes profiles to the observed profiles (T. Yokoyama et al. 2007, in preparation). In this study, we present the line-of-sight (LOS) magnetic field by $B^{\rm LOS} = Bf\cos(\gamma)$, where B is the intrinsic strength of the magnetic field, f is the filling factor, and γ is the inclination with respect to the LOS. We have applied two methods to resolve the 180° azimuth ambiguity: the AZAM utility (Lites et al. 1993) for interactive resolution, and the minimum energy method of Metcalf et al. (2006). However, the azimuth angle (χ) is presented as $\cos(2\chi)$ in this paper. The measure $\cos(2\chi)$ is independent of the resolution of the azimuth ambiguity. SOT, for the first time, revealed sub-arcsecond fine structure of the magnetic field vector around the polarity inversion line at the flare site. With the resolution of this fine structure we encounter new difficulties concerning the resolution of the azimuth ambiguity.

Image co-alignment is necessary for comparing images taken at different times, or at differing wavelengths. When we investigate the relationship between the bright features seen in Ca II H (using the BFI) and the photospheric magnetic fields (using the SP), we determine their relative alignment using an image cross-correlation technique. We cross-correlate the continuum intensity map from the SP with the G-band image taken at the time of midpoint of the closest SP observation. The relationship between the centers of the field-of-view of the G-band and Ca II H images is well known (Shimizu et al. 2007b). The continuum intensity from the SP maps taken at different times are also aligned by image cross-correlation in order to remove any drifts due to satellite jitter, correlation tracking, and sunspot proper motion.

3. Results

3.1. Temporal Change of NOAA 10930 for 7 Days

The active region NOAA 10930 contained a δ-sunspot comprising two umbrae of opposite polarity in apparent "collision" (figure 2). The southern umbra of positive polarity moved from west to east around the large, mature northern umbra of negative polarity (see also movies 1 and 2).* The positive umbra and its immediately surrounding the penumbra rotated counterclockwise. An emerging flux region (EFR1 in the third row of figure 2) appeared at the west side of the positive umbra starting at about 9 UT on December 10. Then, the positive flux merged into the positive umbra, followed by an increase in the size of the positive umbra. Another two flux emergence events (EFR2 and EFR3 in the forth row of figure 2) began at about 0 UT on December 12. The emerging bipole of EFR3 had the same sense as EFR1 (positive–negative oriented east–west), while the emerging bipole of EFR2 was oriented in the sense opposite to the two other EFRs. The negative flux of EFR2 merged into the penumbra surrounding the southern positive umbra, and followed a path around the positive umbra that rotated counterclockwise. As a result, elongated magnetic structures with alternating positive and negative polarities were formed between the two sunspot umbrae. Such elongated magnetic structures were observed at other major flare sites (Zirin & Wang 1993; Wang 2005). The polarity inversion line formed at the boundary of at least 4 magnetic field systems (the two umbrae, EFR1, EFR2, and EFR3) became very complicated before the flare. The elongated magnetic structures gradually disappeared during the day after the X3.4 flare (figure 2q), during which time the polarity inversion line also recovered its less complicated structure.

Many bright loops in the Ca II H images were observed in the collision site between the two umbrae. In particular, the number of Ca II H bright loops suddenly increased during the time when the negative flux of EFR2 entered into the region around the positive umbra (figure 2l). When the X3.4 flare occurred on 2006 December 13, two flare ribbons in Ca II H appeared in the collision site (figure 2o). The duration of the two ribbon flare was about 6 hours.

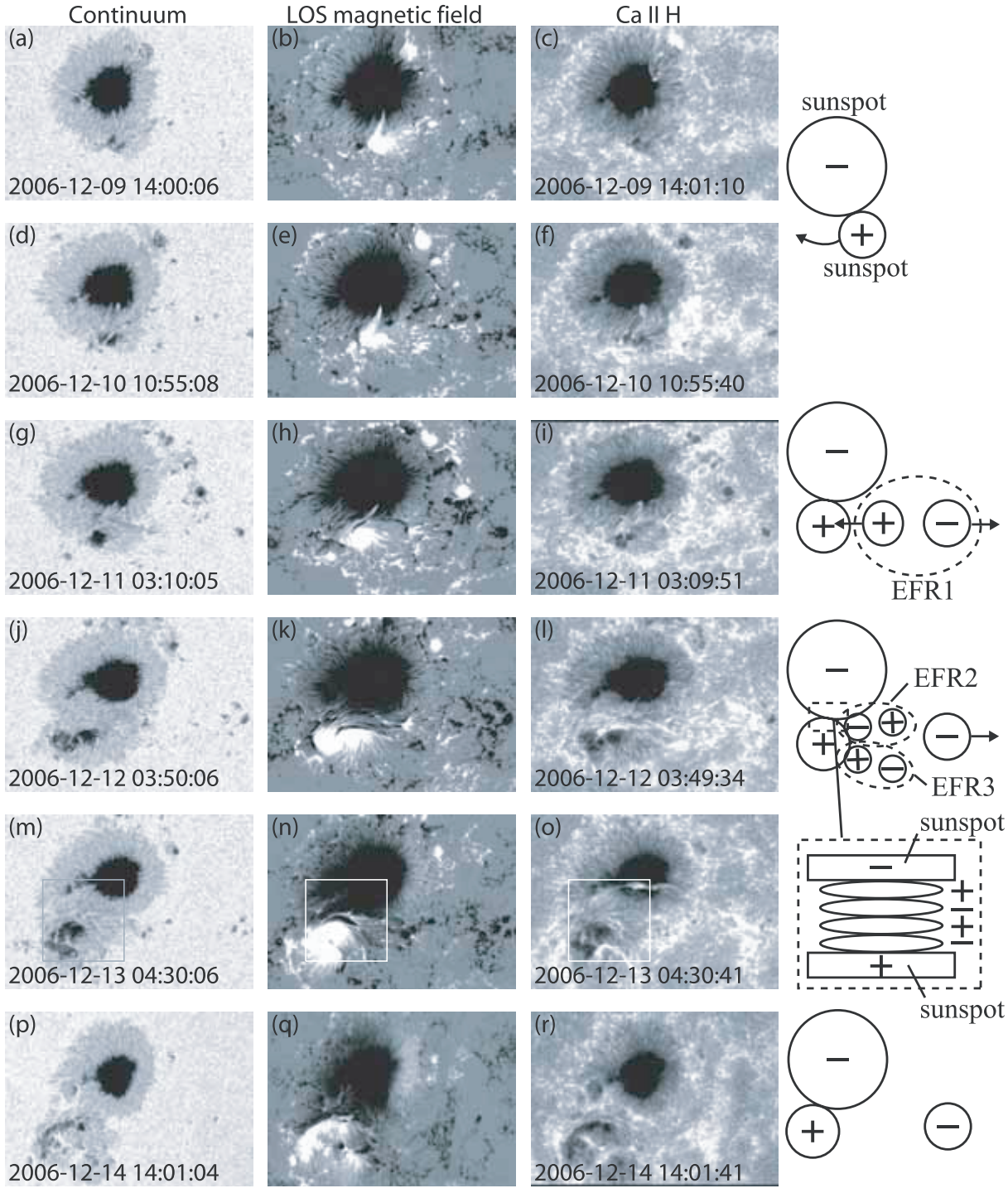

Fig. 2. Day-by-day evolution in NOAA 10930. Continuum intensity and LOS magnetic field maps were obtained with the SOT/SP. Ca II H images were observed with the SOT/BFI. North is up and east is to the left. The field of view is $128'' \times 96''$. The solid boxes indicate the field of view for figures 3 and 4.

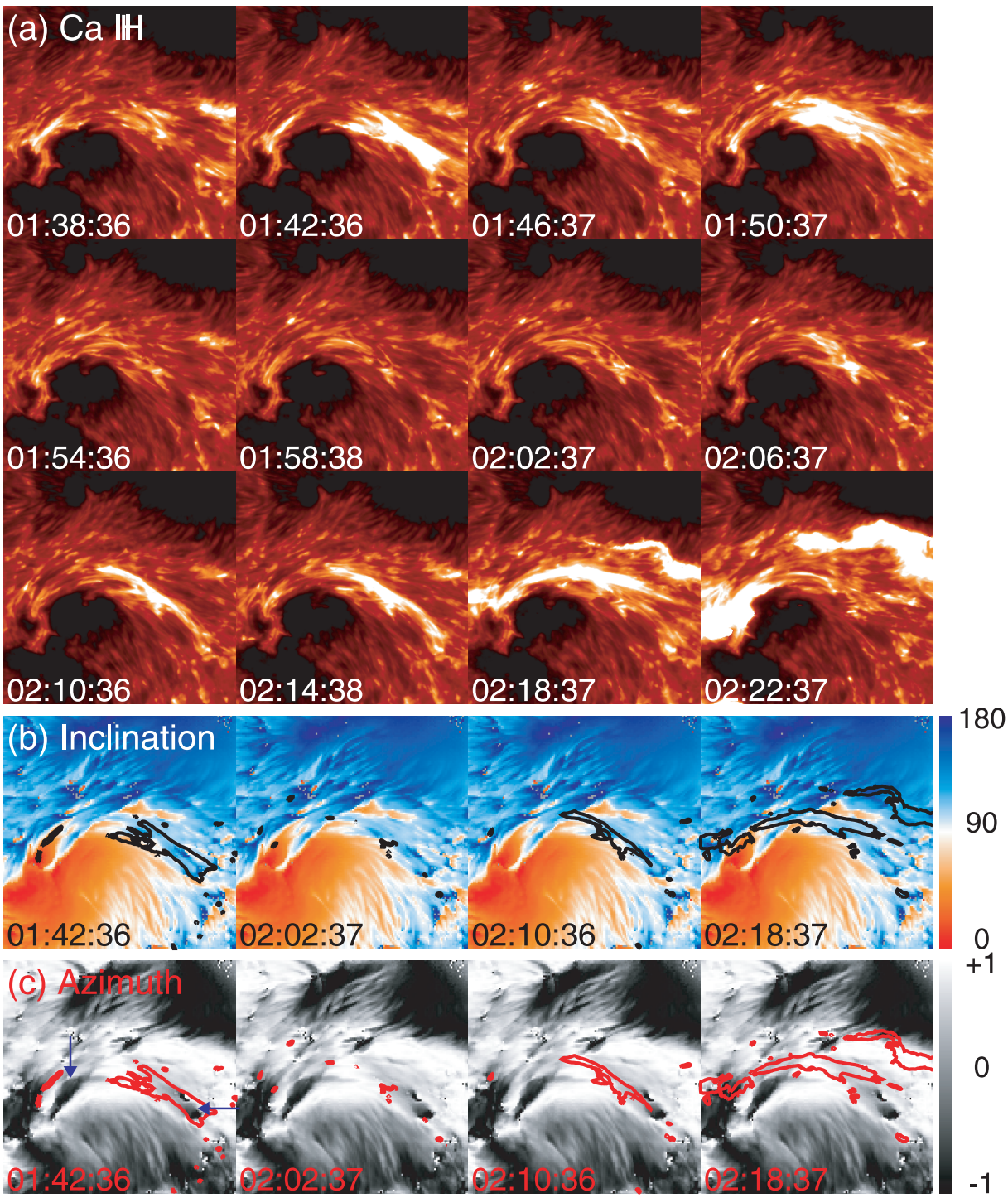

Fig. 3. (a) Time series of Ca II H images observed with the SOT/BFI. (b) Inclination (γ) map, and (c) azimuth (χ) map taken at 20:30–21:33 on December 12 were made from the SOT/SP data. The contours show the Ca II H intensity of 1500 DN. The inclination represents the angle with respect to the LOS direction. An inclination of 90° corresponds to a magnetic field perpendicular to the LOS direction. The azimuth map is represented by a definition of $\cos(2\chi)$. The white area has a magnetic field oriented east–west, while the black area has a magnetic field oriented north–south.

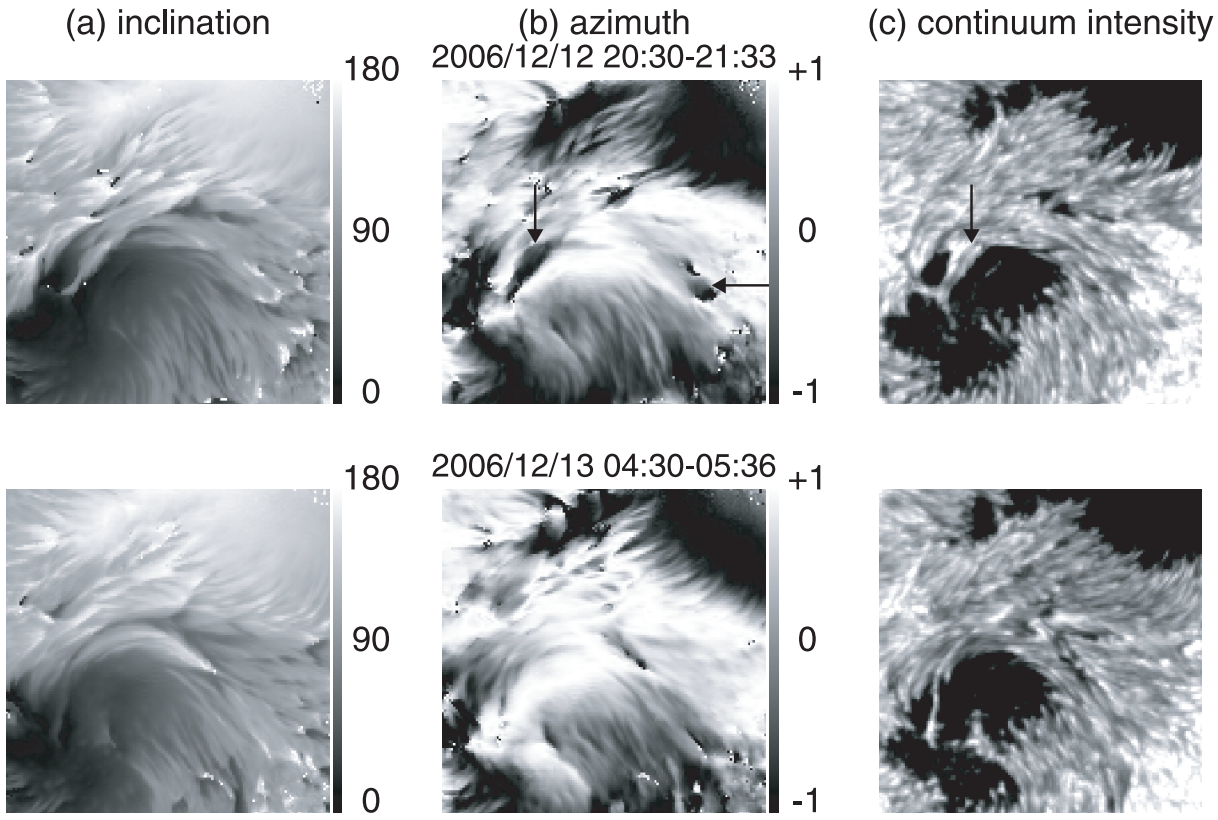

Fig. 4. (a) Inclination map, (b) azimuth map, and (c) continuum intensity map at the flare site. The upper and lower panels were obtained at 20:30–21:33 on December 12 and at 04:30–05:36 on December 13, respectively.

3.2. Photospheric Magnetic Field at the Flare Site

Figure 3a shows the evolution of the two ribbon flare observed in Ca II H. The two ribbon flare starts from a small brightening at 02:02:37 around the polarity inversion line between the two sunspot umbrae (figure 3b). Bright loops having an X-shape appear at 02:10:36, and then they evolve into the southern ribbon of the flare. The southern ribbon and other bright loops, such as observed at 01:42:36, evolve along the polarity inversion line. The two arrows in figure 3c indicate black areas surrounded by white areas in the azimuth map. This means that the magnetic field in the black area is nearly perpendicular to its surroundings. The black areas are located at the polarity inversion line. At least one side of the Ca II H bright loop is rooted at such a black area.

We now examine the temporal change in photospheric magnetic fields at the flare site. The upper and lower panels of figure 4 show magnetic fields taken about 5 hours before and 3 hours after the flare onset, respectively. Some of the complicated polarity inversion lines disappear after the flare, and the polarity inversion line becomes relatively smooth overall (figures 4a). However, the magnetic field structure with alternating polarities still remains between the two sunspots. In the azimuth map, the areas with large azimuth angle with respect to the surroundings (the two arrows in figure 4b) disappear after the flare: white (and gray) areas become dominant around the polarity inversion line. This means that the azimuth angle changes by about 90° in these areas. The penumbra with negative polarity embedded in the southern positive umbra disappears after the flare in one of the areas with a large azimuth angle with respect to the surroundings, as shown by the black arrow in figure 4c.

4. Discussion

Beginning one day before the X3.4 flare, many Ca II H bright loops appeared around the polarity inversion line between the opposite polarity umbrae. Such pre-flare activity near the temperature minimum region was reported as brightening in the UV continuum observed with TRACE (Kurokawa et al. 2002). SOT, for the first time, resolved the brightenings as apparent loops, and some of the bright loops had an X-shaped configuration. The bright loops increased in number during the time that emerging negative elements migrated towards the positive umbra. Therefore, the bright loops were probably the result of magnetic reconnection between the magnetic field lines of the colliding opposite polarity elements.

Many authors showed that rapid and permanent changes of photospheric magnetic fields were associated with large flares (e.g., Wang et al. 1992; Cameron & Sammis 1999; Kosovichev & Zharkova 2001; Spirock et al. 2002; Liu et al. 2005; Sudol & Harvey 2005; Wang 2006). In this flare, there was a one-day gap between the appearance of the elongated magnetic structures with alternating polarities and the X-class flare on December 13. Such elongated magnetic structures

were still observed during the day after the flare. On the other hand, a change in shape of the polarity inversion line and a change in azimuth angle by 90° were observed in small parts of the polarity inversion line at the flare site during an 8-hour interval between successive SP maps before and after onset of the flare. This suggests that, in addition to the variation in the magnetic shear of the whole active region, the temporal change in fine structure of the magnetic fields at the flare site would be related to the trigger mechanism of the major flare. Sudol and Harvey (2005) showed that a typical timescale of the changes in photospheric magnetic fields is less than 10 minutes in 75% of 42 field change sites during 15 X-class flares. Observations of vector magnetic fields with higher cadence are needed to reveal the actual magnetic activity responsible for triggering large solar flares.

We found a change of azimuth angle by 90° in some parts of the polarity inversion line at the flare site. However, there are two possibilities for such a change as a result of the azimuth ambiguity. One is that magnetic fields attain a similar direction to the surrounding fields after the flare; the other is that magnetic fields attain the direction opposite to their surroundings. The magnetic shear at the flare site decreases in the former case and increases in the later case. Moreover, the resolution of the azimuth ambiguity determines the magnetic field configuration of emerging bipoles (U-loop or Ω-loop). The global resolution of azimuth ambiguity may be determined by several algorithms (Metcalf et al. 2006), but it is very difficult to resolve the ambiguity for each of the tiny magnetic elements resolved by SOT. We need to resolve the azimuth ambiguity more carefully when calculating the quantities related to magnetic shear (e.g., magnetic shear angle, magnetic helicity, current density, force-free alpha) from vector magnetic fields.

Hinode is a Japanese mission developed and launched by ISAS/JAXA, with NAOJ as a domestic partner and NASA and STFC (UK) as international partners. It is operated by these agencies in co-operation with ESA and NSC (Norway). The authors would like to express their gratitude to the late Prof. T. Kosugi and all members of the Hinode team for a successful mission. This work was partly carried out at the NAOJ Hinode Science Center, which is supported by the Grant-in-Aid for Creative Scientific Research, "The Basic Study of Space Weather Prediction from MEXT", Japan (Head Investigator: K. Shibata), generous donations from Sun Microsystems, and NAOJ internal funding.

References

Cameron, R., & Sammis, I. 1999, ApJ, 525, L61
Ichimoto, K., et al. 2007, Sol. Phys. submitted
Kosovichev, A. G., & Zharkova, V. V. 2001, ApJ, 550, L105
Kosugi, T., et al. 2007, Sol. Phys., 243, 3
Kurokawa, H., Wang, T., & Ishii, T. T. 2002, ApJ, 572, 598
Lites, B. W., Elmore, D. F., Seagraves, P., & Skumanich, A. P. 1993, ApJ, 418, 928
Liu, C., Deng, N., Liu, Y., Falconer, D., Goode, P. R., Denker, C., & Wang, H. 2005, ApJ, 622, 722
Metcalf, T. R., et al. 2006, Sol. Phys., 237, 267
Priest, E. R., & Forbes, T. G. 2002, A&AR, 10, 313
Shimizu, T., et al. 2007a, Sol. Phys. in press
Shimizu, T., et al. 2007b, PASJ, 59, S845
Spirock, T. J., Yurchyshyn, V. B., & Wang, H. 2002, ApJ, 572, 1072
Sudol, J. J., & Harvey, J. W. 2005, ApJ, 635, 647
Suematsu, Y., et al. 2007, Sol. Phys. submitted
Tsuneta, S., et al. 2007, Sol. Phys. submitted
Wang, H. 2005, ApJ, 618, 1012
Wang, H. 2006, ApJ, 649, 490
Wang, H., Varsik, J., Zirin, H., Canfield, R. C., Leka, K. D., & Wang, J. 1992, Sol. Phys., 142, 11
Zirin, H., & Wang, H. 1993, Nature, 363, 426